

СООБЩЕНИЯ
ОБЪЕДИНЕННОГО
ИНСТИТУТА
ЯДЕРНЫХ
ИССЛЕДОВАНИЙ

ДУБНА



C343e1

G-47

22/x-75

E7 - 8843

P.Gippner

3544/2-75

**EVALUATION OF ELECTRON
AND NUCLEAR BREMSSTRAHLUNG
IN HEAVY ION COLLISIONS**

1975

E7 - 8843

P.Gippner

**EVALUATION OF ELECTRON
AND NUCLEAR BREMSSTRAHLUNG
IN HEAVY ION COLLISIONS**

1. Introduction

At the U-300 heavy ion cyclotron of the Laboratory of Nuclear Reactions Kaun and coworkers have measured the quasimolecular KX-ray emission obtained in the collision systems ${}_{32}^{74}\text{Ge} + {}_{32}^{74}\text{Ge}$ (81 MeV)^{/1/}; Zr, Nb, Mo, Rh + ${}_{41}^{93}\text{Nb}$ (65 MeV, 96 MeV)^{/2,3/}; La + ${}_{57}^{139}\text{La}$ (115 MeV)^{/4/} and La + ${}_{54}^{132,136}\text{Xe}$ (120 MeV, 150 MeV)^{/4/}.

Till now only Meyerhof et al.^{/5/} and Greenberg et al.^{/6/} have reported similar experiments in the region of mean atomic numbers Z . There is a considerable interest in observing X-rays from quasiautomatic systems transiently formed in heavy ion bombardments of targets of various atomic numbers. The detection of quasimolecular X-radiation provides the possibility of investigating the electron shells of superheavy elements with $Z > 110$ ^{/7/} and of studying in the future quantum electrodynamical effects in strong fields^{/8/}. However, a lot of other effects, e.g., electronic and nuclear bremsstrahlung, radiative electron capture, two-quanta decay and Compton scattering of γ -rays occur as competing effects in these measurements^{/9/}. It is the purpose of this paper to describe calculations, which allow to estimate the contributions of the electronic and nuclear bremsstrahlung to the X-ray spectra measured in references^{/2,3/}. The calculations for bremsstrahlung due to secondary electrons were carried out using the theory of Folkmann et al.^{/10/}, while for nuclear bremsstrahlung calculations the theory of Alder et al.^{/11/} was used. Such calculations are of current interest not only regarding the aspects of atomic physics described above but also with

respect to measurements in ion induced X-ray analysis, where bremsstrahlung of secondary electrons and nuclear bremsstrahlung highly contribute to the background radiation. Therefore, similar evaluations can serve for an optimization of the ratio effect/background in such investigations /11, 12/.

2. Electronic Bremsstrahlung

2.1. The Differential Cross Section

According to ref. /10/ the differential cross section for production of bremsstrahlung from secondary electrons by impact of heavy ions (E_1, Z_1, A_1) with target atoms (Z_2, A_2) is given by the formula

$$\frac{d\sigma^b(E_r, E_1)}{dE_r} = \int_{E_r}^{\infty} dE_{\delta} \frac{d\sigma_e(E_{\delta}, E_1)}{dE_{\delta}} \cdot \frac{dY(E_{\delta}, E_r)}{dE_r}, \quad (1)$$

where $\frac{d\sigma_e(E_{\delta}, E_1)}{dE_{\delta}}$ is the differential cross section for production of secondary electrons in the energy interval $[E_{\delta}, E_{\delta} + dE_{\delta}]$ by an ion with the incidence energy E_1 , and $\frac{dY(E_{\delta}, E_r)}{dE_r}$ is the yield of bremsstrahlung in the X-ray energy interval $[E_r, E_r + dE_r]$, induced by an δ -electron of an energy $E_{\delta} > E_r$.

As is shown in ref. /10/, the yield is given by

$$\frac{dY(E_{\delta}, E_r)}{dE_r} = \int_{E_r}^{E_{\delta}} \frac{d\sigma_r(E_e, E_r)}{dE_r} \cdot \frac{dE_e}{m_e M_p A_2 S_2(E_e)}. \quad (2)$$

In this formula $\frac{d\sigma_r(E_e, E_r)}{dE_r}$ is the differential cross section for production of bremsstrahlung in the energy

interval $[E_r, E_r + dE_r]$ for an electron with an energy E_e , $m_e \cdot M_p \cdot A_2 = m_2$ is the mass of a target atom ($m_e =$ electron mass, $M_p = 1836.6$), and $S_2(E_e)$ is the stopping power in energy per mass for the electrons

in the target material. Hence, the expression $\frac{dE_e}{m_e M_p A_2 S_2(E_e)}$

stands for the number of atoms per unit area colliding with the electron along the electron path and corresponding to the energy loss dE_e of the electron.

By inserting equation (2) into (1) one obtains for the cross section of secondary electron bremsstrahlung

$$\frac{d\sigma^b(E_r, E_1)}{dE_r} = \int_{E_r}^{\infty} dE_{\delta} \frac{d\sigma_e(E_{\delta}, E_1)}{dE_{\delta}} \int_{E_r}^{E_{\delta}} \frac{d\sigma_r(E_e, E_r)}{dE_r} \cdot \frac{dE_e}{m_e M_p A_2 S_2(E_e)}. \quad (3)$$

As it is done in Folkmann's work /10/ the cross section

$\frac{d\sigma_e(E_{\delta}, E_1)}{dE_{\delta}}$ for production of secondary electrons in

heavy ion impact was calculated by means of the binary encounter approximation of Garcia et al. /13/ assuming the dominant interaction producing the inner-shell ionization to be a direct energy exchange between the projectile and the atomic electron in question. In the framework of this approximation one obtains for the ionization cross section of bound s -shell electrons

$$\frac{d\sigma_e(E_{\delta}, E_1)}{dE_{\delta}} = \int_0^{\infty} \frac{d\sigma(\Delta E, v_1, v_2)}{dE_{\delta}} f(v_2) dv_2, \quad (4)$$

where $\frac{d\sigma(\Delta E, v_1, v_2)}{dE_{\delta}}$ is the cross section for the

exchange of an energy $\Delta E = U_s + E_{\delta}$ between the incident ion and the bound s -electron, whose velocity is v_2 and whose energy is $E_2 = \frac{1}{2} m_e v_2^2$. U_s is the binding energy on the s -shell.

For the various cases of energy transfer ΔE this cross section is given by the expressions /13/

$$\frac{d\sigma(\Delta E, v_1, v_2)}{dE_\delta} = \frac{\pi}{3} \cdot \frac{(Z_1 e^2)^2}{(\Delta E)^3} \cdot \frac{3v_2'^2 + v_2^2}{v_1^2}, \quad 0 \leq \Delta E < b, \quad (5a)$$

$$= \frac{\pi}{6} \cdot \frac{(Z_1 e^2)^2}{(\Delta E)^3} \cdot \frac{(v_1 + v_1')^3 + (v_2 - v_2')^3}{v_1^2 v_2}, \quad b \leq \Delta E < a \quad (5b)$$

$$= \frac{\pi}{3} \cdot \frac{(Z_1 e^2)^2}{(\Delta E)^3} \cdot \frac{v_1'(v_1'^2 + 3v_1^2)}{v_1^2 v_2}, \quad a \leq \Delta E, \quad (5c)$$

$$2m_e v_2 > (m_1 - m_e) v_1$$

$$= 0, \quad a \leq \Delta E, \quad (5d)$$

$$2m_e v_2 < (m_1 - m_e) v_1$$

where

$$a = \frac{4m_1 m_e}{(m_1 + m_e)^2} [E_1 - E_2 + \frac{1}{2} v_1 v_2 (m_1 - m_e)],$$

$$b = \frac{4m_1 m_e}{(m_1 + m_e)^2} [E_1 - E_2 - \frac{1}{2} v_1 v_2 (m_1 - m_e)], \quad (6)$$

$$v_1' = [v_1^2 - \frac{2\Delta E}{m_1}]^{1/2} \text{ and } v_2' = [v_2^2 + \frac{2\Delta E}{m_e}]^{1/2}.$$

In order to calculate the cross section $\frac{d\sigma_e(E_\delta, E_1)}{dE_\delta}$ using

formula (4) one has to integrate over all velocities v_2 which occur on the electron shell with the principal quantum number s . In this integration we used the Fock distribution

$$f(v_2) = \frac{32v_0^5}{\pi} \cdot \frac{v_2^2}{(v_2^2 + v_0^2)^4}, \quad v_0 = [\frac{2U_s}{m_e}]^{1/2}, \quad (7)$$

as a normalized weight function.

2.2. Numerical Calculations

The program BINARY enables one to evaluate the following quantities:

1. the cross section $\frac{d\sigma_e}{dE_\delta}$ corresponding to (4) and (5) for production of secondary electrons,
2. the cross section $\frac{d\sigma^b}{dE_r}$ for bremsstrahlung production, corresponding to formula (3),
3. the spectra $\frac{dN^b(E_r, E_1)}{dE_r}$ for bremsstrahlung, corresponding to formula (8),

4. the "measured" spectra $\epsilon(E_r) \frac{dN^b(E_r, E_1)}{dE_r}$, where $\epsilon(E_r)$ represents the efficiency of the detector used including the absorber attenuation.

The integrations in (3) and (4) were carried out using existing subroutines. For the expressions $\frac{d\sigma_r}{dE_r}$ and

$\frac{dE_e}{m_e M_p A_2 S_2(E_e)}$ we have employed the approxi-

mations made by Folkmann et al.^{/10/}. Further, with regard to the forward peaking of the ejected electrons and the angular distribution of the measured bremsstrahlung we have taken into account the assumptions made in ref.^{/10/}.

The cross section (4) were multiplied by the number a_s of electrons occupying a shell s and summed over the shells of interest. Further, the slowing-down^{/14/} of the ions in the target materials used was considered.

For that purpose we supposed the targets to consist of N foils of equal thickness. Assuming a constant ion energy E_i inside each foil, for a target placed at 45° with respect to the beam direction the bremsstrahlung spectra are given by

$$\frac{dN^b(E_r, E_i)}{dE_r} = \sum_{i=1}^N N_{ION} n_i e^{-\mu(E_r) R_i} \sum_{s=1}^{\nu} a_s \frac{d\sigma_s^b(E_r, E_i)}{dE_r}, \quad (8)$$

where N_{ION} is the number of incident ions and n_i is the number of atoms per cm^2 inside a target foil. Finally, the factor $\exp[-\mu(E_r) R_i]$ takes into consideration the absorption for X-radiation of an energy E_r inside the target. The infinite upper integration limits in expressions (3) and (4) have been substituted by finite limits in the following way:

As can be seen from formula (5d) the integrand in (4) vanishes if $a < \Delta E$ and $2m_e v_2 < (m_1 - m_e) v_1$. Hence, one obtains from (3)

$$\int_{E_r}^{\infty} dE_\delta \frac{d\sigma_e(\Delta E)}{dE_\delta} = \int_{E_r}^{\Delta E_{max} - U_s} dE_\delta \frac{d\sigma_e(\Delta E)}{dE_\delta}, \quad \Delta E_{max} = a.$$

For the evaluation of ΔE_{max} we reexamine relation (5d). Taking into account $m_1 = m_e M_p \cdot A_1$ one obtains from $2m_e v_2 < (m_1 - m_e) v_1$ after division

$$\text{by } v_0 = \left[\frac{2U_s}{m_e} \right]^{1/2}$$

$$\frac{v_2}{v_0} < \frac{M_p A_1 - 1}{2} \left[\frac{E_i}{M_p A_1 U_s} \right]^{1/2}. \quad (9)$$

On the other hand the condition $a < \Delta E$ is consistent with the inequality

$$\left(\frac{v_2}{c} \right)^2 - \frac{v_2}{c} (M_p A_1 - 1) \left[\frac{2E_i}{M_p A_1 \cdot 0.511} \right]^{1/2} + \frac{2}{0.511} \left[\frac{(M_p A_1 + 1)^2}{4M_p A_1} \Delta E - E_i \right] = a > 0, \quad (10)$$

($E_i, \Delta E$ in MeV), yielding finally after division by v_0

$$\left(\frac{v_2}{v_0} \right)_{+/-} = \frac{M_p A_1 - 1}{2} \left[\frac{E_i}{M_p A_1 U_s} \right]^{1/2} \pm \frac{M_p A_1 + 1}{2} \left[\frac{E_i - \Delta E + a'}{M_p A_1 U_s} \right]^{1/2}. \quad (11)$$

$\left(\frac{v_2}{v_0} \right)_+$ is in contradiction to (9), therefore for our purposes only $\left(\frac{v_2}{v_0} \right)_-$ solves the inequality (10) well.

Then the quantity ΔE_{max} is defined by $a' = 0$ and by using (11) one gets

$$\Delta E_{max} = E_i - M_p A_1 U_s \left[\frac{M_p A_1 - 1}{M_p A_1 + 1} \left[\frac{E_i}{M_p A_1 U_s} \right]^{1/2} - \frac{2}{M_p A_1 + 1} \cdot \frac{v_2}{v_0} \right]^2. \quad (12)$$

Now, the integration of equation (4) will be divided by the velocity $v_2 = \left(\frac{v_2}{v_0} \right)_- \cdot v_0$ into two parts of which only

the integral with the limits $[0, \left(\frac{v_2}{v_0} \right)_- \cdot v_0]$ gives

a contribution. The values ΔE_{max} for K-shells evaluated by (12) belonging to different quantities $\left(\frac{v_2}{v_0} \right)_-$ are shown in the table.

Table
 E_{max} / keV as a function of the upper integration limit v_2/v_0 in (4). The binding energies of the K-shells used are evaluated in accordance with the Slater rules /16/.

reaction v_2/v_0	C+p $E_1 = 3MeV$	Al+p $E_1 = 3MeV$	Nb+Nb $E_1 = 65MeV$
10	33.7	71.1	105.9
20	60.7	134.9	213.3
30	87.6	198.2	320.6
40	114.3	260.6	423.8

3. Evaluation of Nuclear Bremsstrahlung

In ref. /11/ it is demonstrated that the E1 component of nuclear bremsstrahlung has the highest intensity and the contributions of higher electrical multiplicities can be neglected*. The differential cross section of this component is

$$\frac{d\sigma_{E1}^b(E_r, E_1)}{dE_r} = 1.225 \times 10^{-8} Z_1^2 Z_2^2 \left[\frac{Z_1}{A_1} - \frac{Z_2}{A_2} \right]^2 \frac{A_1}{E_1 \cdot E_r} f_{E1}(\eta, \xi), \quad (13)$$

where η is a collision parameter defined by

$$\eta = \frac{Z_1 Z_2}{2} \left[\frac{A_1}{10.008 E_1} \right]^{1/2} \quad (E_1 \text{ in MeV})$$

and ξ is an adiabaticity parameter

$$\xi = \frac{Z_1 Z_2 A_1^{1/2} E_r'}{12.65 (E_1 - \frac{1}{2} E_r')^{3/2}} \left[1 + \frac{5}{32} \left(\frac{E_r'}{E_1} \right)^2 + \dots \right]$$

with the abbreviation $E_r' = (1 + A_1/A_2) E_r$. The values for $f_{E1}(\eta, \xi)$ are given in ref. /11/, table II.3, in the classical approximation $\eta \rightarrow \infty$. For all practical purposes, the approximation can be used if $\eta \geq 100$ (ref. /11, 13/). Under the experimental conditions described in ref. /2, 3/ for the investigation of the reactions Zr, Nb, Mo, Rh + Nb (65 MeV, 96 MeV) this relation was fulfilled. The factor $\left(\frac{Z_1}{A_1} - \frac{Z_2}{A_2} \right)^2$ in formula

(13) indicates that in a closed system of particles characterized by $\frac{Z_i}{A_i} = \text{const.}$ no electrical dipole radiation can arise. Higher multiplicities will be important but with much slower intensity and the energy loss of the incident ions is caused only by recoil effects and ionization processes.

*This includes also the neglect of interference effects.

The dipole bremsstrahlung is anisotropic. The angular distribution for this radiation induced by incident ions is

$$W_{E1}(\theta) = 1 + \frac{1}{4} a_2^{E1} (3 \cos^2 \theta - 1), \quad (14)$$

where θ is the angle between the beam direction and the bremsstrahlung quanta measured. The coefficients $a_2^{E1} (\eta > 100, \xi)$ used are given in ref. /15/. The cross section (13) was calculated by the program CONTI making use of interpolation between the values $f_{E1}(\eta, \xi)$ given in ref. /11/. For the evaluation of $f_{E1}(\eta, \xi)$ in the limits $\xi \rightarrow 0$ and $\xi \gg 1$ asymptotic formulae were utilized /11/. Taking into account the significant slowing-down of the ions in the targets used, as mentioned above, we supposed the targets to consist of a number of N thin foils. By assuming a constant ion energy E_1 inside each foil for a target in 45 geometry, one obtains for the spectra of the nuclear bremsstrahlung

$$\frac{dN_{E1}^b(E_r, E_1)}{dE_r} = \sum_{i=1}^N N_{ION} n_i e^{-\mu(E_r) R_i} \frac{d\sigma_{E1}^b(E_r, E_1)}{dE_r}. \quad (15)$$

4. Results

For the reactions Al + p (2 MeV) and Al + p (3 MeV) in figures 1a and 1b we compare the differential cross sections for bremsstrahlung evaluated using (8) and (15) with the results obtained by Folkmann et al. /10/. Figures 2a and 2b contain the comparison of the cross sections for the collision systems C + p (3 MeV) and C + p (5 MeV) (ref. /12/). These figures should be a good proof for the correct work of our programs.

For the upper integration limit in formula (4) we have chosen $v_2 = 40 v_0$ (see the table). The influence of any higher integration limits is of the same order of magnitude as the errors of the subroutines used for the integration. For the binding energies U_s we have employed the values according to the Slater rules /16/.

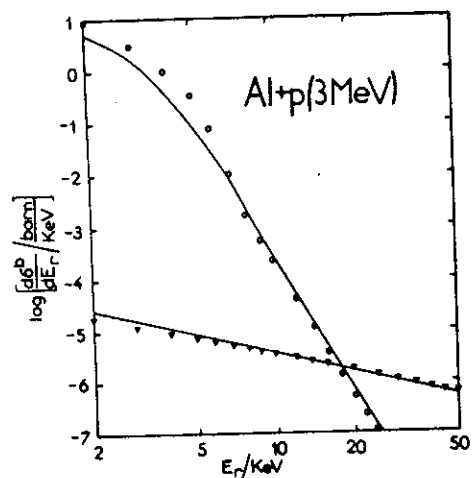
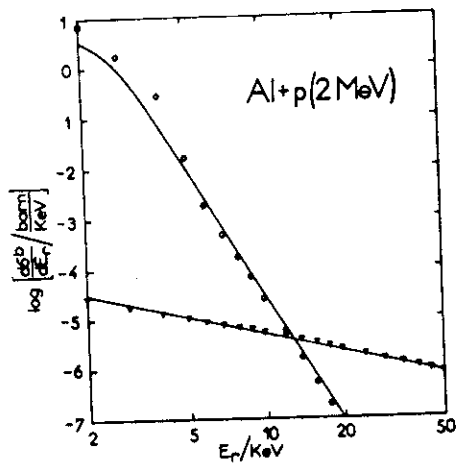


Fig. 1a,b: The cross sections $\frac{d\sigma^b(E_r)}{dE_r}$ for bremsstrahlung of secondary electrons (upper, parabolic curve) and nuclear bremsstrahlung (lower curve) in the reactions $\text{Al} + p$ (2 MeV) and $\text{Al} + p$ (3 MeV). The full lines are the results of Folkmann et al. /10/, the triangles and circles represent the cross sections for nuclear and electronic bremsstrahlung, respectively, computed with the programs CONTI and BINARY.

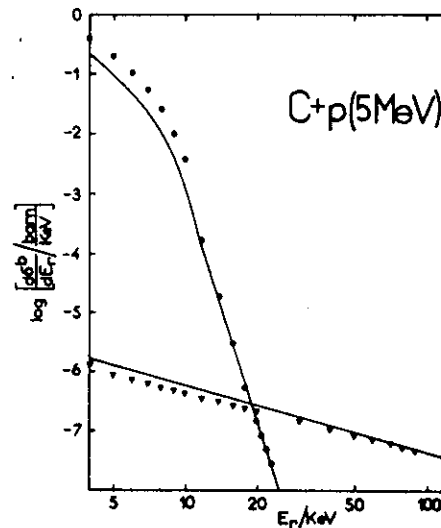
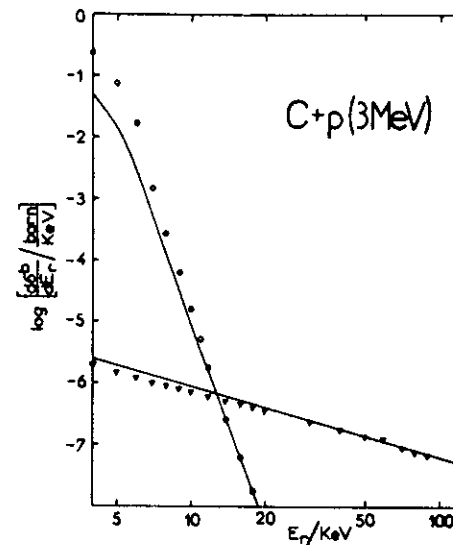


Fig. 2a,b: The cross sections $\frac{d\sigma^b(E_r)}{dE_r}$ for bremsstrahlung of secondary electrons (upper, parabolic curve) and nuclear bremsstrahlung (lower curve) in the reactions $\text{C} + p$ (3 MeV) and $\text{C} + p$ (5 MeV). The full lines denote the results of Folkmann et al. /12/. For the explanation of the other symbols see figs. 1a,b.

The contributions $\epsilon(E_r) \frac{dN^b(E_r)}{dE_r}$ of both electro-

nic and nuclear bremsstrahlung to the X-ray continua measured in the reactions Zr, Nb, Mo, Rh + Nb (65 MeV)^{/2/} are illustrated in fig. 3. The triangles denote the spectrum of the E1 component of nuclear bremsstrahlung, the dashed line shows the summed spectrum of electronic and nuclear bremsstrahlung. In the colliding system Nb + Nb no E1 component can arise. Therefore, the dashed line illustrates only the contribution of electronic bremsstrahlung. Fig. 4 shows the bremsstrahlung continua obtained in the reaction Zr, Nb, Mo + Nb (96 MeV)^{/3/}. The X-ray spectra are normalized to the same ion flux. The triangles and circles represent the spectra of the nuclear and electronic bremsstrahlung, respectively, whereas the dashed-dotted line represents the mean background measured in a delayed regime^{/3/}. Finally the dashed line gives the summed spectrum of bremsstrahlung and delayed background.

Figures 3 and 4 demonstrate that contrary to the supposition made in ref.^{/2/} the low energy parts (C1) of the X-ray continua cannot be explained as due to the bremsstrahlung of secondary electrons. The yield integral computed for the X-ray energy range between 16 keV and 30 keV is at least three orders of magnitude smaller than the values measured^{/2,3/}. Also the slope is wrong. After correcting for the detector efficiency and absorber attenuation the linear extrapolation of the spectra (C1) in a logarithmic representation shows that the experimental yield Y(C1) goes down like E_r^{-n} with $n \approx 20$. This disagrees drastically with the value $n \leq 7$ obtained using formula (8). Taking into account the results of references^{/17/} it seems possible to explain the feature of the continua (C1) by the static approximation of the atomic collisions, whereas the continua (C2), which may extend beyond the united atom limit, may be caused by dynamic effects. Further theoretical and experimental investigations are needed to provide evidence for the molecular origin of both conspicuous continua.

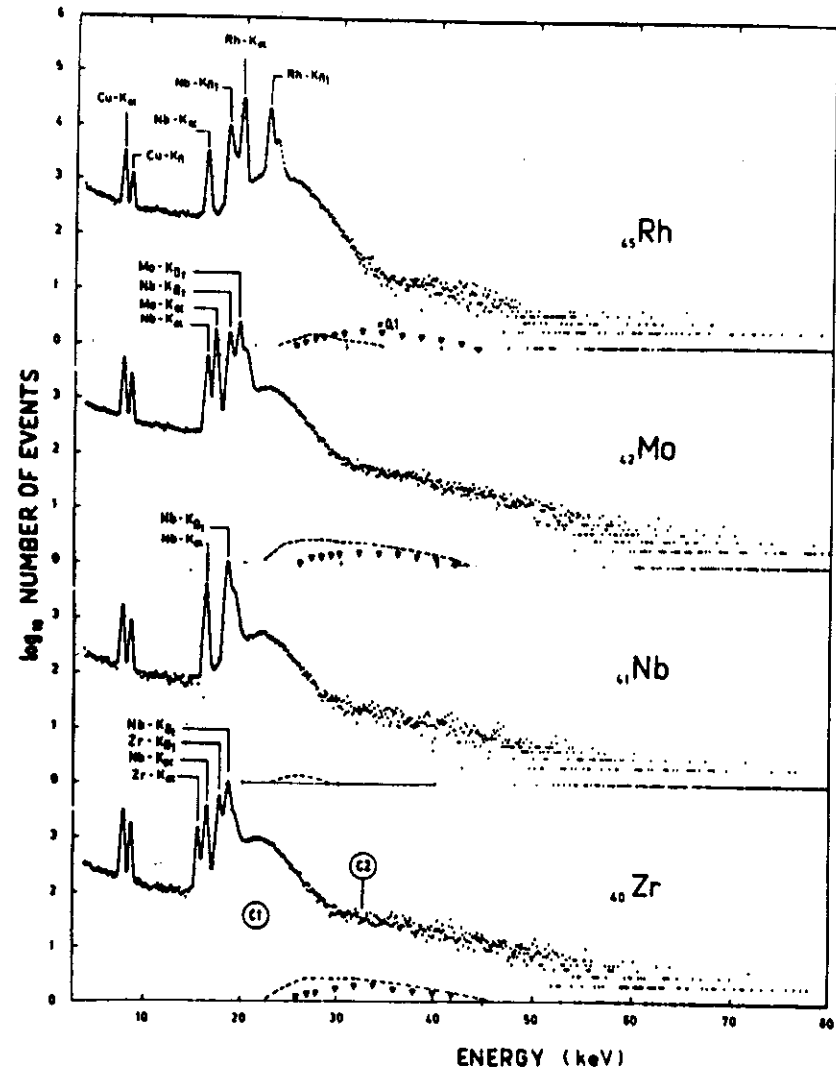


Fig. 3. The contributions of bremsstrahlung to the X-ray continua measured in the reactions Zr, Nb, Mo, Rh + Nb (65 MeV)^{/2/}. The triangles denote the spectrum of the E1 component of nuclear bremsstrahlung only, whereas the dashed line represents the summed spectrum of electronic and nuclear bremsstrahlung.

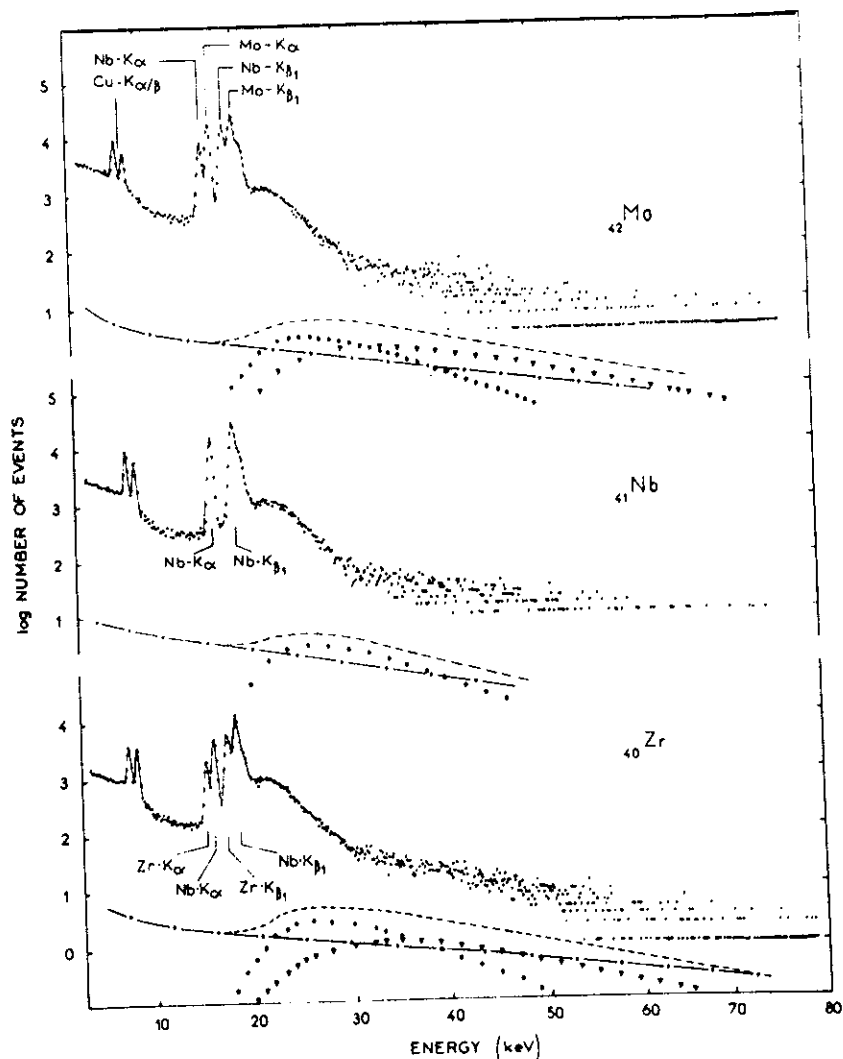


Fig. 4. The contributions of bremsstrahlung to the X-ray continua obtained in the reactions $Zr, Nb, Mo + {}^93Nb$ (96 MeV)^{13/}. The dashed-dotted line represents the mean background measured in a delayed regime^{13/}. The triangles and circles denote the spectra of nuclear and electronic bremsstrahlung, respectively. The dashed line is the summed spectrum of delayed background and bremsstrahlung.

For the collision systems (target, p) the results of Folkmann's theory were improved by the experiment^{12/}, whereas for the systems (target, HI) one expects theoretical cross sections to be slightly smaller than those measured. In these cases one must consider additionally the bremsstrahlung due to the bound electrons ejected from the incident ions. The ionization cross sections for the electron shells of these ions can be computed by formulae (4) - (7) in a system, where the ions are at rest and the

target atoms have a kinetic energy $E_1' = E_1 \cdot \frac{m_2}{m_1}$. These

cross sections were not calculated but their inclusion is highly unlikely to account for the high yields $Y(C1)$ observed^{2,3/}.

The author would like to thank Academician G.N.Flerov for his support to this work and Dr. K.-H.Kaun for helpful discussions.

References

1. P.Gippner, K.-H.Kaun, F.Stary, W.Schulze, Y.P.Tretyakov. *Nucl. Phys.*, A230, 509 (1974).
2. P.Gippner, K.-H.Kaun, H.Sodan, F.Stary, Y.P.Tretyakov. *Phys.Lett.*, 52B, 183 (1974).
3. W.Frank, P.Gippner, K.-H.Kaun, W.Schulze, H.Sodan, Y.P.Tretyakov. *JINR*, E7-8616, Dubna, 1975.
4. W.Frank, P.Gippner, K.-H.Kaun, W.Schulze, Y.P.Tretyakov. *ZFK-283*, annual report 1974, p. 62.
5. W.E.Meyerhof, T.K.Saylor, S.M.Lazarus, W.A.Little, B.B.Triplett, L.F.Chase (Jr.). *Phys.Rev.Lett.*, 30, 1279 (1973) and *Phys.Rev.Lett.*, 32, 502 (1974).
6. C.K.Davis, J.S.Greenberg. *Phys.Rev.Lett.*, 32, 1215 (1974). *J.S.Greenberg, C.K.Davis, P.Vincent. Phys. Rev.Lett.*, 33, 473 (1974).
7. B.Müller, R.K.Smith, W.Greiner. *Spectroscopy of Superheavy Two Centre Orbitals*, to be published.
8. B.Müller, J.Rafelski, W.Greiner. *Z.Phys.*, 257, 183 (1972). *J.Rafelski, L.P.Fulcher, W.Greiner. Phys. Rev.Lett.*, 27, 958 (1971). *V.S.Popov. Sov. Phys., JETP*, 32, 526 (1971).
9. F.W.Saris. Invited talk at the 5th Int. Conf. on Collisions in Solids, Gatlinburg 1973.

10. F.Folkmann, C.Gaarde, T.Huus, K.Kemp. *Nucl.Instr. Meth.*, 116, 487 (1974).
11. K.Alder, A.Bohr, T.Huus, B.Mottelson, A.Winther. *Rev.Mod.Phys.*, 28, 432 (1956).
12. F.Folkmann, J.Borggreen, A.Kjeldgaard. *Nucl.Instr. Meth.*, 119, 117 (1974).
13. J.D.Garcia. *Phys.Rev.*, 117, 223 (1969).
J.D.Garcia. *Phys.Rev.*, A1, 280 (1970).
14. L.C.Northcliffe, R.F.Schilling. *Nucl. Data Tables*, A7, 233 (1970).
15. R.M.Thaler, M.Goldstein, J.L.McHale, L.C.Biedenharn. *Phys.Rev.*, 102, 1567 (1956).
16. J.C.Slater. *Phys.Rev.*, 36, 57 (1930).
17. J.S.Briggs. *J.Phys. B: Atom. Molec. Phys.*, 7, 47 (1974).

*Received by Publishing Department
on May 4, 1975.*